Article

Extracellular Matrix Tunes the Regenerative Potential of Fetal Stem Cells

Yixuan Amy Pei , Jhanvee Patel , Ming Pei *

Posted Date: 15 December 2023

doi: 10.20944/preprints202312.1155.v1

Keywords: fetal stem cells; decellularized extracellular matrix; differentiation; fetal nucleus pulposus cell; fetal synovium-derived stem cell

Article

Extracellular Matrix Tunes the Regenerative Potential of Fetal Stem Cells

Yixuan Amy Pei [1,2], Jhanvee Patel [1] and Ming Pei [1,3,*]

[1] Stem Cell and Tissue Engineering Laboratory, Department of Orthopaedics, West Virginia University, Morgantown, WV, USA; mpei@hsc.wvu.edu (M.P.); Yixuan.Pei@Pennmedicine.upenn.edu (Y.A.P.)
[2] Perelman School of Medicine at the University of Pennsylvania, Philadelphia, PA, USA
[3] WVU Cancer Institute, Robert C. Byrd Health Sciences Center, West Virginia University, Morgantown, WV, USA
* Correspondence: mpei@hsc.wvu.edu; Tel.: +1-304-293-1072

Abstract: Adult mesenchymal stem cells (MSCs) are a promising cell source for tissue regeneration. However, ex vivo expansion results in cell senescence; cells lose their proliferation and differentiation capacity. Fetal MSCs can be an alternative due to their robust proliferation and differentiation capacities as well as immune privilege properties. Given the rejuvenation effect of decellularized extracellular matrix (dECM) on adult MSCs, it remains unknown whether dECM influences the regenerative potential of fetal stem cells. In this study, passage five fetal nucleus pulposus cells (fNPCs) and fetal synovium-derived stem cells (fSDSCs) were expanded on dECMs deposited by fNPCs (NECM) and fSDSCs (SECM) for one passage with expansion on tissue culture plastic (Plastic) as a control. We found that dECM expanded fNPCs and fSDSCs exhibited both similarities and differences in expression of stemness genes and surface markers. Expanded fNPCs yielded more differentiated pellets after chondrogenic induction but no adipogenic differentiation following adipogenic induction in both Plastic and dECM groups than the corresponding fSDSC group. Despite a significant increase in fNPCs, dECM expanded fSDSCs exhibited no increase in chondrogenic potential; however, compared to the Plastic group, dECM expanded fSDSCs exhibited a small increase in osteogenic potential and a great increase in adipogenic potential. These results suggest that fNPCs are more sensitive to NECM rejuvenation for cartilage tissue engineering and regeneration; in contrast, dECMs exhibited limited effects on fSDSC rejuvenation in chondrogenic capacity except for enhanced adipogenic capacity following expansion on SECM.

Keywords: fetal stem cell; decellularized extracellular matrix; differentiation; fetal nucleus pulposus cell; fetal synovium-derived stem cell

1. Introduction

Adult mesenchymal stem cells (MSCs) are a promising cell source for tissue engineering and regeneration [1]. However, cell senescence due to either donor age and/or ex vivo expansion becomes a challenge for the application of MSCs in clinical treatment [2]. Compared to adult MSCs with median levels of human leukocyte antigen (HLA) class I and low levels of HLA class II, fetal MSCs have low levels of HLA class I and do not express HLA class II, indicating that fetal MSCs have greater immunomodulatory properties [3–5]. Moreover, fetal MSCs possess higher proliferation and differentiation capacities than adult MSCs, indicating fetal MSCs may be advantageous for MSC-based tissue regeneration [6–9].

Despite adult MSCs being prone to aging during ex vivo expansion, decellularized extracellular matrix (dECM) deposited by MSCs provides a solution to rejuvenate both proliferation and chondrogenic capacity in adult MSCs [10,11]. There is an abundance of research supporting the use of cell-derived dECM to maintain stemness, prevent cell senescence, and limit oxidative stress when expanding stem cells [12–16]. Previously, we found that human adult synovium-derived MSCs (aSDSCs) were rejuvenated after expansion on dECM deposited by fetal SDSCs (fSDSCs) compared to that deposited by aSDSCs [17]. Furthermore, high-passage (senescent) infrapatellar fat pad-

 doi:10.20944/preprints202312.1155.v1

derived MSCs (IPFSCs) grown on dECM deposited by low-passage (young) IPFSCs gained greater proliferative and chondrogenic capacity, whereas high-passage IPFSCs expanded on dECM deposited by high-passage IPFSCs lost their proliferative and chondrogenic potential [18], indicating that matrix microenvironment can greatly influence adult MSC regenerative potential. This evidence could also suggest that dECM deposited by younger, more proliferative cells could have greater ability for rejuvenation [17,18].

However, it remains unknown whether a fetal matrix microenvironment can influence the regenerative potential of fetal stem cells. In this study, two fetal MSCs, including SDSCs, a tissue-specific stem cell for chondrogenesis [19], and nucleus pulposus cells (NPCs), a chondrogenic progenitor cell [20], were used to characterize fetal MSCs in expression of stemness genes and surface markers, proliferation capacity, as well as chondrogenic, adipogenic, and osteogenic potential following expansion on dECMs deposited by fSDSCs (SECM) or fetal NPCs (fNPCs) (NECM). Major matrix proteins were also assessed for expression in dECMs deposited by fSDSCs and fNPCs as well as in expanded cells and multi-differentiated fetal MSCs.

2. Materials & Methods

2.1. Human fNPC and fSDSC culture

Human fNPCs and fSDSCs were seeded into T175 tissue culture plastic (Plastic) flasks at 3000 cells/cm^2 in complete medium [α-minimum essential medium (α-MEM) supplemented with 10% fetal bovine serum (FBS), 100 U/mL penicillin, 100 μg/mL streptomycin, and 0.25 μg/mL fungizone) (Thermo Fisher Scientific, Waltham, MA, USA)]. The cells were cultured in a 5% CO_2 incubator at 37^{o}C with the medium changed every other day. During expansion, cell number was measured and morphology was documented.

2.2. Preparation of dECMs

Plastic flasks were pre-coated with 0.2% gelatin from bovine skin, type B (Milipore Sigma, St. Louis, MO, USA) at 37^{o}C for 1 hour followed by treatment with 1% glutaraldehyde solution (Thermo Fisher Scientific) and 1M ethanolamine (Milipore Sigma) at room temperature for 30 minutes each. Passage 4 (P4) fSDSCs and fNPCs were seeded on pre-coated Plastic flasks (3800 cells/cm^2). After reaching 100% confluence, cells were cultured and treated with 250 μM L-ascorbic acid phosphate (Wako Chemicals USA Inc., Richmond, VA, USA) diluted in the culture medium for an additional 10 days. Then, the cells were incubated with lysis buffer containing 0.5% Triton X-100 (Milipore Sigma) and 20 mM ammonium hydroxide (Milipore Sigma) at 37^{o}C for 10 minutes. After cell removal, dECMs were kept in phosphate buffered solution (PBS)-diluted lysis buffer (1:1) at 4^{o}C for overnight. The next day, the dECMs were washed with PBS and stored in PBS containing 100 U/mL penicillin, 100 μg/mL streptomycin, and 0.25 μg/mL fungizone at 4^{o}C until use.

2.3. Evaluation of proliferation, surface markers, and stemness genes of expanded fSDSCs and fNPCs

P5 fSDSCs and P5 fNPCs were expanded on Plastic and dECMs deposited by fSDSCs and fNPCs, respectively, for one passage, subsequently followed by the analyses below.

Expanded cells were assessed for cell proliferation using nucleoside analogue Click-iT EdU (5-ethynyl-2′-deoxyuridine) Alexa Flour™ 647 Flow Cytometry Assay Kit (Invitrogen, Eugene, OR, USA). After expanded cells reached 45% confluence, EdU was added to the cell culture medium at a final concentration of 10 μM. After 20 hours of incubation, harvested cells (3×10^5 each group) were washed twice in PBS containing 1% bovine serum albumin (BSA) and fixed in 180 μL of Click-iT™ fixative (0.4% paraformaldehyde). After 15 minutes of incubation at room temperature in the dark, cells were washed two times in 1x Click-iT™ saponin-based permeabilization and wash buffer. Cell samples then were incubated with Click-iT™ reaction cocktail (1x) at room temperature in the dark for 30 minutes and washed three times with 1x Click-iT™ saponin-based permeabilization and wash buffer. Fluorescence was detected by a BD FACSCalibur™ flow cytometer (BD Biosciences, San Jose,

Preprints (www.preprints.org) | NOT PEER-REVIEWED | Posted: 15 December 2023 doi:10.20944/preprints202312.1155.v1

CA, USA). The FCS Express 7 Research Edition (De Novo software, Los Angeles, CA, USA) was used for data analysis.

Expanded cells (4×10^5 each group) were first incubated in cold PBS containing 0.1% ChromPure Human IgG, whole molecule (Jackson ImmunoResearch Laboratories, West Grove, PA, USA) for 30 minutes. Then, the cells were incubated in the dark with primary antibodies at 4°C for 30 minutes. Primary antibodies used in this study are listed in **Table 1**. Fluorescence was analyzed by a BD FACSCalibur™ flow cytometer (BD Biosciences). Data analysis was performed by the FCS Express 7 Research Edition (De Novo software).

Total RNAs from samples (n = 3) extracted using Trizol® (Millipore Sigma) were quantified and about 2 micrograms of total RNA were used for reverse transcription with High-Capacity cDNA Reverse Transcription Kit at 37°C for 120 minutes as recommended by the manufacturer (Thermo Fisher Scientific). TaqMan® real-time quantitative polymerase chain reaction (qPCR) was used to evaluate expression of stemness-related genes (*MYC*, *KLF4*, *BMI1*, *POU5F1*, *NES*, *NOV*, *NANOG*, *SOX2*), adipogenic-related genes (*LPL*, *FABP4*, *CEBPA*), osteogenic-related genes (*BGLAP*, *ALPL*, *COL1A1*), and chondrogenic marker-related genes (*SOX9*, *ACAN*, *Col2A1*, *PRG4*, *FBLN1*, *FOXF1*). *GAPDH* was carried out as the endogenous control gene. TaqMan® Assay IDs of primers are listed in **Table 2**. Each experiment was repeated three times using Applied Biosystems™ 7500 Fast Real-Time PCR System (Applied Biosystems, Waltham, MA, USA). The cycle parameters were 50°C for 2 minutes, hot start at 95°C for 10 minutes followed by 40 cycles of denaturation at 95°C for 15 seconds, and annealing and extension at 60°C for 1 minute. Relative transcript levels were calculated as $\chi = 2^{-\Delta\Delta Ct}$, in which $\Delta\Delta Ct = \Delta E - \Delta C$, $\Delta E = Ct_{exp} - Ct_{GAPDH}$, and $\Delta C = Ct_{ct1} - Ct_{GAPDH}$.

Table 1. Primary antibodies used in surface marker analysis.

Antibody	Company information	Concentration	Catalog no.
CD73 Monoclonal Antibody (AD2), APC, human	eBioscience™, Fisher Scientific, Waltham, MA, USA	0.125 μg/test	17-0739-42
Anti-CD146 Monoclonal Antibody (P1H12) PE, human	eBioscience™, Fisher Scientific	0.125 μg/test	12-1469-42
PE anti-human SSEA-4	BioLegend, Dedham, MA, USA	0.125 μg/test	330406
CD90-APC-Vio® 770, human	Miltenyi Biotec, San Diego, CA, USA	2 μL/test	130-114-863
CD105-PerCp-Vio® 700, human	eBioscience™	2 μL/test	130-112-170

Table 2. TaqMan® assay ID information of target genes for qPCR.

Gene name	Full name	TaqMan® assay ID
	Stemness-related genes	
MYC	MYC proto-oncogene	Hs00153408_m1
KLF4	Kruppel-like factor 4	Hs00358836_m1
BMI1	B lymphoma Mo-MLV insertion region 1 homolog	Hs00180411_m1
POU5F1	POU class 5 homeobox 1	Hs04260367_gH
NES	Nestin	Hs04187831_g1
NOV	Nephroblastoma overexpressed	Hs00159631_m1
NANOG	Nanog homeobox	Hs02387400_g1
SOX2	SRY-box2	Hs01053049_s1
	Adipogenesis-related genes	
LPL	Lipoprotein lipase	Hs00173425_m1
FABP4	Fatty acid-binding protein 4	Hs01086177_m1
CEBPA	CCAAT/enhancer-binding protein alpha	Hs00269972_s1
	Osteogenesis-related genes	

 doi:10.20944/preprints202312.1155.v1

BGLAP	Bone gamma-carboxyglutamate protein	Hs01587814_g1
ALPL	Alkaline Phosphatase, Liver	Hs01029144_m1
COL1A1	Type I collagen	Hs00164004_m1
	Chondrogenesis-related genes	
SOX9	SRY-Box 9	Hs00165814_m1
ACAN	Aggrecan	Hs00153936_m1
Col2A1	Type II collagen	Hs00156568_m1
PRG4	Proteoglycan 4	Hs00981633_m1
FBLN1	Fibulin 1	Hs00972609_m1
FOXF1	Forkhead Box F1	Hs00230962_m1
	Housekeeping internal gene	
GAPDH	Glyceraldehyde-3-phosphate dehydrogenase	Hs02758991_g1

2.4. Immunofluorescence staining of dECMs

The dECMs on pre-coated tissue culture coverslips were blocked with 1% BSA (Thermo Fisher Scientific) at room temperature for 1 hour and incubated with primary antibodies against varied antigens (**Table 3**). Anti-collagen IV (COL4), fibronectin (FN1), and nidogens 1 and 2 (NID1 and NID2) were detected using Alexa Fluor Plus 555-conjugated anti-mouse secondary antibodies (Invitrogen). Anti-laminin (LAMA) and anti-perlecan (PLC) were detected by Alexa Flour 488-conjucated anti-rabbit (Invitrogen) and Alexa Flour 488-conjucated anti-rat (Invitrogen) secondary antibodies, respectively. Fluorescent intensity was visualized under a Zeiss Axiovert 40 CFL Inverted Microscope (Zeiss Oberkochen, Germany) using 20× objective lens.

Table 3. Primary antibodies used in immunofluorescence staining of dECMs.

Antibody	Catalog no.	Company	Species	Working conc.
Collagen II	II6B3-c	Developmental Studies	Mouse	3 µg/mL
Collagen IV	M3F7	Hybridoma Bank (	Mouse	3 µg/mL
Fibronectin	HFN 7.1	DSHB), Iowa City, IA, USA	Mouse	3 µg/mL
Laminin	PA1-16730	Invitrogen, Waltham, MA, USA	Rabbit	20 µg/mL
Col1A1 (3G3)	sc-293182		Mouse	1 µg/mL
Perlecan (A7L6)	sc-33707	Santa Cruz Biotechnology,	Rat	4 µg/mL
Nidogen 1 (C-7)	sc-133175	Inc., Dallas, TX, USA	Mouse	2 µg/mL
Nidogen-2 (F-2)	sc-377424		Mouse	2 µg/mL

2.5. Induction and assessment of adipogenesis, osteogenesis, and chondrogenesis

For chondrogenic induction, 0.3 × 10^6 expanded cells from each group were centrifuged at 1,200 rpm for 7 minutes in a 15-mL polypropylene tube to make a pellet. After 24 hours of incubation in complete medium, D0 pellets were collected. The remaining pellets were cultured in a serum-free chondrogenic induction medium consisting of high-glucose Dulbecco's Modified Eagle's medium (DMEM), 40 µg/mL proline (Millipore Sigma), 100 µM dexamethasone (Millipore Sigma), 100 U/mL penicillin, 100 µg/mL streptomycin, 0.1 mM ascorbic acide-2-phosphate (Wako Chemicals), and 1 × ITS™ Premix (6.25 µg/mL insulin, 6.25 µg/mL transferrin, 6.25 µg/mL selenous acid, 5.35 µg/mL linoleic acid, and 1.25 µg/mL BSA, from BD Biosciences) with the supplementation of 10 ng/mL transforming growth factor beta 3 (TGF-β3; PeproTech Inc., Rocky Hill, NJ, USA) in a 37°C, 5% O_2, 5% CO_2 humidified incubator for 21 days. Chondrogenic differentiation was evaluated using histology and immunohistochemistry (IHC) analyses as well as qPCR targeting chondrogenic-related genes (**Table 2**). For histology, the representative pellets (n = 3) were fixed in 4% paraformaldehyde at 4°C overnight, followed by dehydration in a gradient ethanol series, clearing with xylene, and embedding in paraffin blocks. For histological staining, 5-µm-thick sections were stained with Alician

 doi:10.20944/preprints202312.1155.v1

blue (Thermo Fisher Scientific) and counterstained with fast red for sulfated glycosaminoglycan (GAG). For IHC analysis, the consecutive sections were hydrated, treated with 1% hydrogen peroxide to inhibit endogenous peroxidase, and incubated for 30 minutes with 2 mg/mL hyaluronidase in PBS (pH 5) at 37°C followed by another 30 minutes with 1% normal horse serum and then were probed with primary antibodies against types of collagen I (Genetex, Irvine, CA, USA) and collagen II (Developmental Studies Hybridoma Bank, DSHB, Iowa City, IA, USA) followed by secondary antibody of biotinylated horse anti-mouse/rabbit IgG (H+L) (Vector, Burlingame, CA, USA). Immunoactivity was detected using Vectastain ABC reagent (Vector) with 3, 3′-diaminobenzidine (DAB, Vector) as a substrate. Counterstaining was done with hematoxylin (Vector).

Expanded cells seeded in T25 flasks were incubated in adipogenic induction cocktail, which was complete medium supplemented with 1 μM dexamethasone (Millipore Sigma), 0.5 mM isobutyl-1-methylxanthine (Thermo Fisher Scientific), 200 μM indomethacin (Millipore Sigma), and 10 μM insulin (BioVendor, Asheville, NC, USA) in a 37°C incubator containing 5% CO_2. For staining of the lipid-filled droplets inside the cells after 21 days induction, samples (n = 3) were fixed in 4% formaldehyde for 30 minutes and then stained with fresh 0.6% (w/v) Oil Red O (ORO) (Milipore Sigma) solution (60% isopropanol, 40% water) for 30 minutes at room temperature on the shaker. After washing to remove unbound dye, stained cells were observed under an Olympus IX51 microscope (Olympus America Inc., Center Valley, PA, USA). Adipogenic marker gene expression was quantified using qPCR (**Table 2**).

Expanded cells grown in T25 flasks were incubated in osteogenic induction medium, which was complete medium supplemented with 10 nM dexamethasone (Millipore Sigma), 50 mg/L L-ascorbic acid-2-phosphate (Wako Chemicals), and 10 mM β-glycerophosphate (Glycerol 2-phosphate disodium salt hydrate) (Millipore Sigma) in a 37°C incubator containing 5% CO_2 for an additional 21 days. For assessment of calcium deposition and matrix mineralization, induced cells (n = 3) were fixed with 4% cold formaldehyde for 30 minutes and then incubated in 1% Alizarin Red S (ARS) solution (pH = 4.3; Millipore Sigma) for 20 minutes at room temperature with agitation on the shaker. After rinsing with PBS, images of calcium deposition were taken using an Olympus IX51 microscope (Olympus America Inc.). Osteogenic marker gene expression was quantified using qPCR (**Table 2**).

2.6. Statistical analysis

Results from qPCR are presented as the mean and standard deviation of the mean (Mean ± SD); the Mann–Whitney U test was used for pairwise comparison. All statistical analyses were performed with SPSS 20.0 statistical software (SPSS Inc., Chicago, IL, USA). $p < 0.0.5$ was considered statistically significant.

3. Results

3.1. Assessment of stemness-related gene expression in fetal stem cells after expansion on dECMs

After preparation of dECMs (**Figure 1A**), fetal MSCs seeded on either Plastic or dECMs for one day exhibited polarized distribution (**Figure 1B**). qPCR analysis (**Figure 1C**) showed that fNPCs exhibited less expression of *SOX2*, *NANOG*, *POU5F1*, *NES*, and *KLF4* than fSDSCs except for expression of *NOV*, *MYC*, and *BMI1*. dECM expansion dramatically increased mRNA levels of *SOX2*, *NANOG*, *POU5F1*, *NOV*, and *NES* in fNPCs, particularly for the first four genes in the SECM group and the last one in the NECM group. Interestingly, dECM expansion diminished expression of *SOX2*, *NANOG*, *POU5F1*, *NOV*, and *KLF4* but increased expression of *NES* and *MYC* in fSDSCs. Despite less response of fNPCs to dECM expansion in expression of *KLF4* and *MYC*, fSDSCs exhibited an upregulation of *MYC* expression following dECM expansion, particularly for the NECM group.

Preprints (www.preprints.org) | NOT PEER-REVIEWED | Posted: 15 December 2023 doi:10.20944/preprints202312.1155.v1

Figure 1

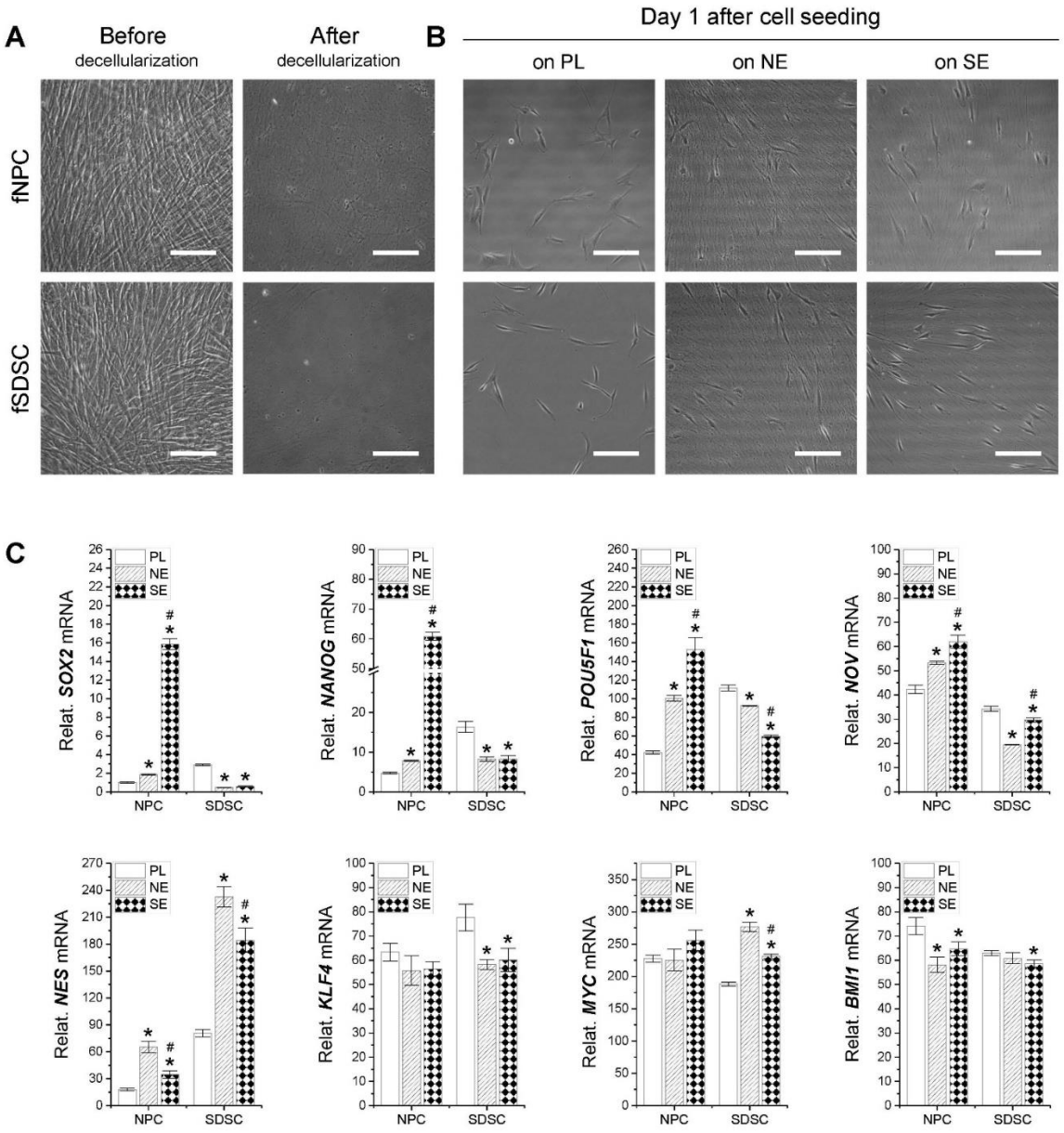

Figure 1. Fetal MSC morphology and stemness gene expression following expansion on dECMs. (**A**) Before and after decellularization of ECMs deposited by fNPCs and fSDSCs. Scale bar: 100 μm. (**B**) Cell morphology of fetal MSCs after expansion on dECMs deposited by fNPCs (NE) or fSDSCs (SE) with tissue culture plastic (PL) as a control. Scale bar: 100 μm. (**C**) Assessment of stemness gene expression including *SOX2*, *NANOG*, *POU5F1*, *NOV*, *NES*, *KLF4*, *MYC*, and *BMI1* in fNPCs and fSDSCs following expansion on NE, SE, or PL using TaqMan® real-time qPCR. *GAPDH* serves as the internal control. Data shown as a bar chart. * indicates a statistically significant difference from the corresponding PL group ($p < 0.05$). # indicates a statistically significant difference from the corresponding NE group ($p < 0.05$).

3.2. Assessment of surface marker expression in fetal stem cells after expansion on dECMs

To characterize surface marker expression and evaluate cell proliferation capacity, flow cytometry was used to measure surface phenotypes CD73, CD90, CD105, CD146, and SSEA4 as well as relative EdU incorporation in fetal stem cells following expansion on dECMs (**Figure 2**). We found that the percentage of CD73, CD90, CD146, and SSEA4 in fSDSCs remained stable in the range

Preprints (www.preprints.org) | NOT PEER-REVIEWED | Posted: 15 December 2023 doi:10.20944/preprints202312.1155.v1

between 97% and 100% after growth on dECMs. In the fNPC groups, CD73 and CD90 remained stable in similar levels to the fSDSC groups. However, the percentage of CD146 was 95% in the Plastic group, which dropped to 65% in the NECM group and 82% in the SECM group. Interestingly, the percentage of SSEA4 was 50% in the PL group and increased to 65% in the NECM group and 78% in the SECM group. The above data indicate that fSDSCs exhibit higher expression of MSC surface markers and less response to dECM expansion compared to fNPCs. Intriguingly, median fluorescent intensity (MFI) in both fetal stem cells showed the same trend in response to dECM expansion. Following expansion on dECMs, the MFI of CD73 and SSEA4 increased while that of CD90 and CD146 decreased. Compared to a different response of fNPCs and fSDSCs in the percentage of CD105 expression, dECM expansion increased relative EdU incorporation in both fetal cells, particularly for the SECM group.

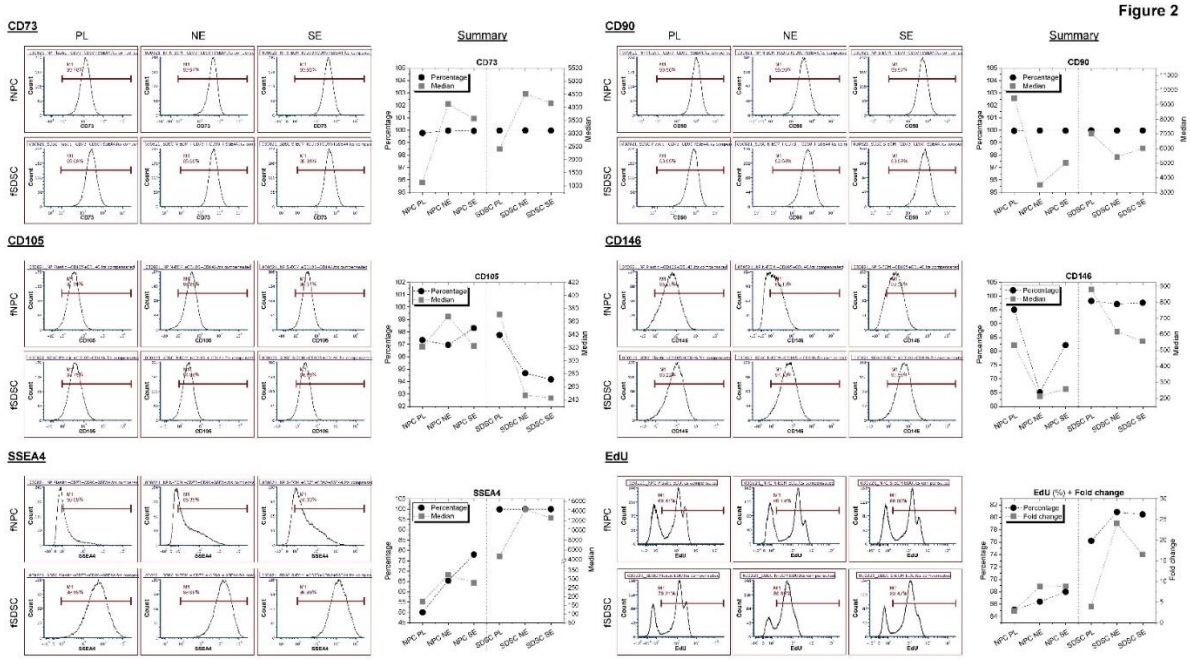

Figure 2. Assessment of fetal MSC surface marker expression following expansion on dECMs. Flow cytometry was used to measure expression of MSC surface markers CD73, CD90, CD105, CD146, and SSEA4 as well as relative EdU incooperation in fNPCs and fSDSCs following expansion on dECM deposited by fetal NPCs (NE) or fetal SDSCs (SE) with tissue culture plastic (PL) as a control.

3.3. Chondrogenic capacity of fetal stem cells after growth on dECMs

To characterize the chondrogenic potential of fetal MSCs following expansion on dECMs, P5 fSDSCs and fNPCs grown on SECM and NECM were incubated in a pellet culture system toward chondrogenesis. After 21-day chondrogenic induction, qPCR data showed that fNPCs exhibited greater response to chondrogenic induction than fSDSCs. fNPCs yielded higher expression of *ACAN*, *COL2A1*, and *PRG4* but lower expression of *COL1A1* and *COL10A1* after expansion on NECM; fSDSCs yielded lower expression of *ACAN* and *COL1A1* and higher expression of *COL2A1* and *COL10A1* after expansion on SECM (**Figure 3A**). Compared to Plastic expansion, interestingly, dECM expanded fNPCs exhibited a decrease in *FBLN1* (a marker for human articular cartilage) while an increase in *FOXF1* (a marker for human NP tissue) [21], particularly for NECM; dECM expanded fSDSCs displayed no significant change in *FBLN1* and *FOXF1* (**Figure 3B**).

Compared to Plastic expansion, dECM expanded fNPCs yielded significantly larger pellets while dECM expanded fSDSCs did not have much change (**Figure 3C**). dECM expanded fNPCs yielded pellets with more intense staining of sulfated GAGs and collagen II and less staining of collagen I than the Plastic group; dECM expanded fSDSCs yielded pellets with similar intensity of the staining to the Plastic group (**Figure 3C**).

Preprints (www.preprints.org) | NOT PEER-REVIEWED | Posted: 15 December 2023 doi:10.20944/preprints202312.1155.v1

Figure 3

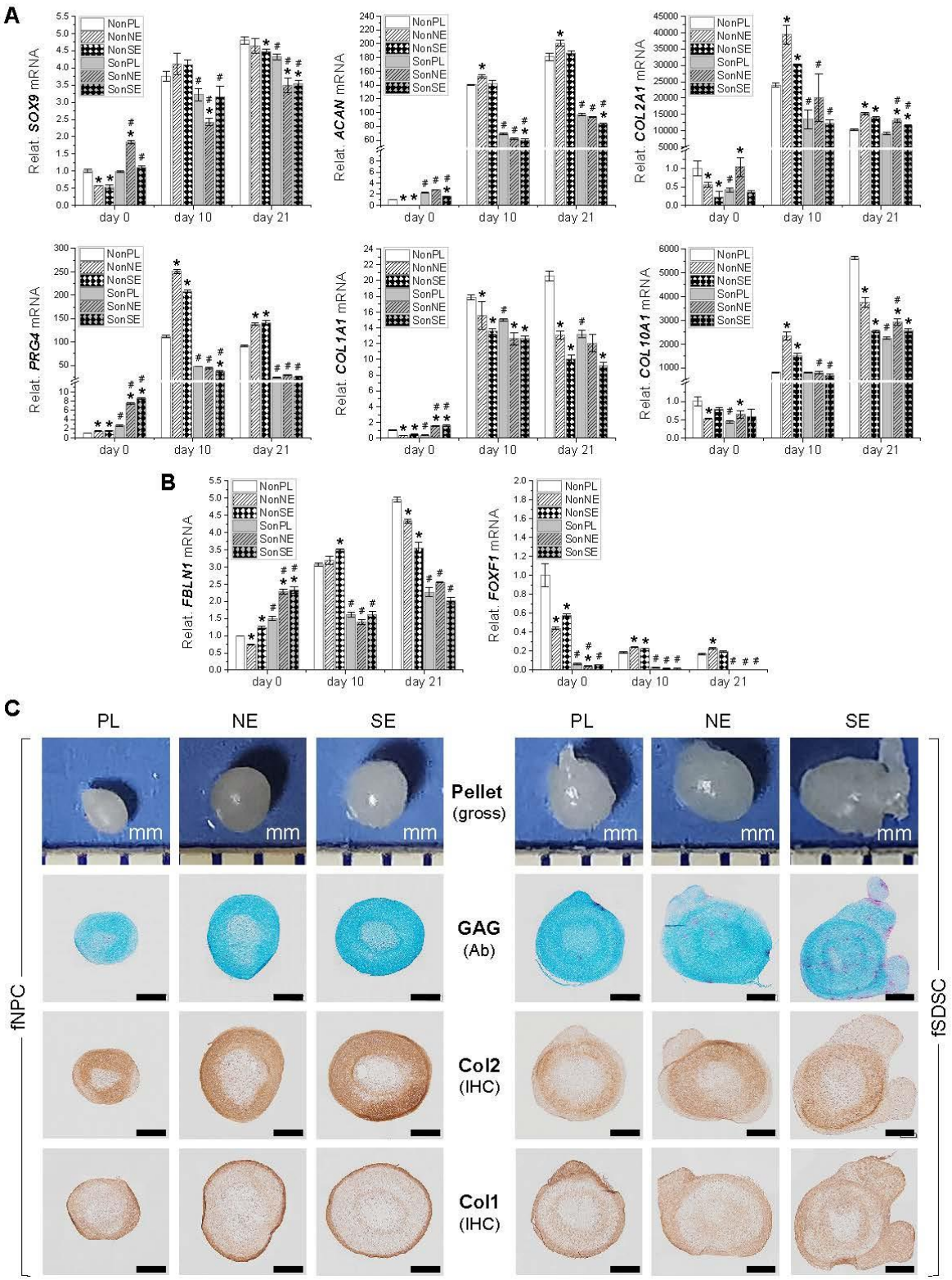

Figure 3. Chondrogenic evaluation of fetal MSCs following expansion on dECMs. fNPCs (N) and fSDSCs (S) following expansion on dECMs deposited by fNPCs (NE) or fSDSCs (SE) or tissue culture plastic (PL) were incubated in a pellet culture system with chondrogenic medium for 21 days. TaqMan® real-time PCR was used to evaluate chondrogenic marker genes *SOX9*, *ACAN*, *COL2A1*, *PRG4*, *COL1A1*, and *COL10A1* (**A**), and *FBLN1* and NPC marker gene *FOXF1* (**B**) in the pellets collected at days 0, 10, and 21 after chondrogenic induction. *GAPDH* serves as the internal control.

Preprints (www.preprints.org) | NOT PEER-REVIEWED | Posted: 15 December 2023 doi:10.20944/preprints202312.1155.v1

Data shown as a bar chart. * indicates a statistically significant difference from the corresponding PL group ($p < 0.05$). # indicates a statistically significant difference from the corresponding fNPC group ($p < 0.05$). (**C**) Alcian blue staining (Ab) was used to detect sulfated GAGs and immunohistochemistry staining (IHC) was used to detect collagen I (COL1) and collagen II (COL2). Scale bar: 400 μm.

3.4. Adipogenic capacity of fetal stem cells after growth on dECMs

To characterize the adipogenic potential of fetal MSCs following expansion on dECMs, P5 fSDSCs and fNPCs grown on SECM and NECM for one passage were incubated toward adipogenesis for 21 days. qPCR data (**Figure 4A**) showed that, following adipogenic induction, fNPCs exhibited less expression/response than the corresponding fSDSCs. Compared to Plastic expansion, fSDSCs grown on SECM exhibited significantly greater levels of *LPL*, *FABP4*, and *CEBPA* whereas fSDSCs grown on NECM only displayed a higher level of *FABP4*. fNPC groups displayed no significant increases in any adipogenic marker gene expression. These trends are supported by assessment of adipogenic markers at the protein level, such as PLIN2 and FABP4 by Western blot (**Figure 4B**) and lipid droplets by ORO staining (**Figure 4C**).

Figure 4

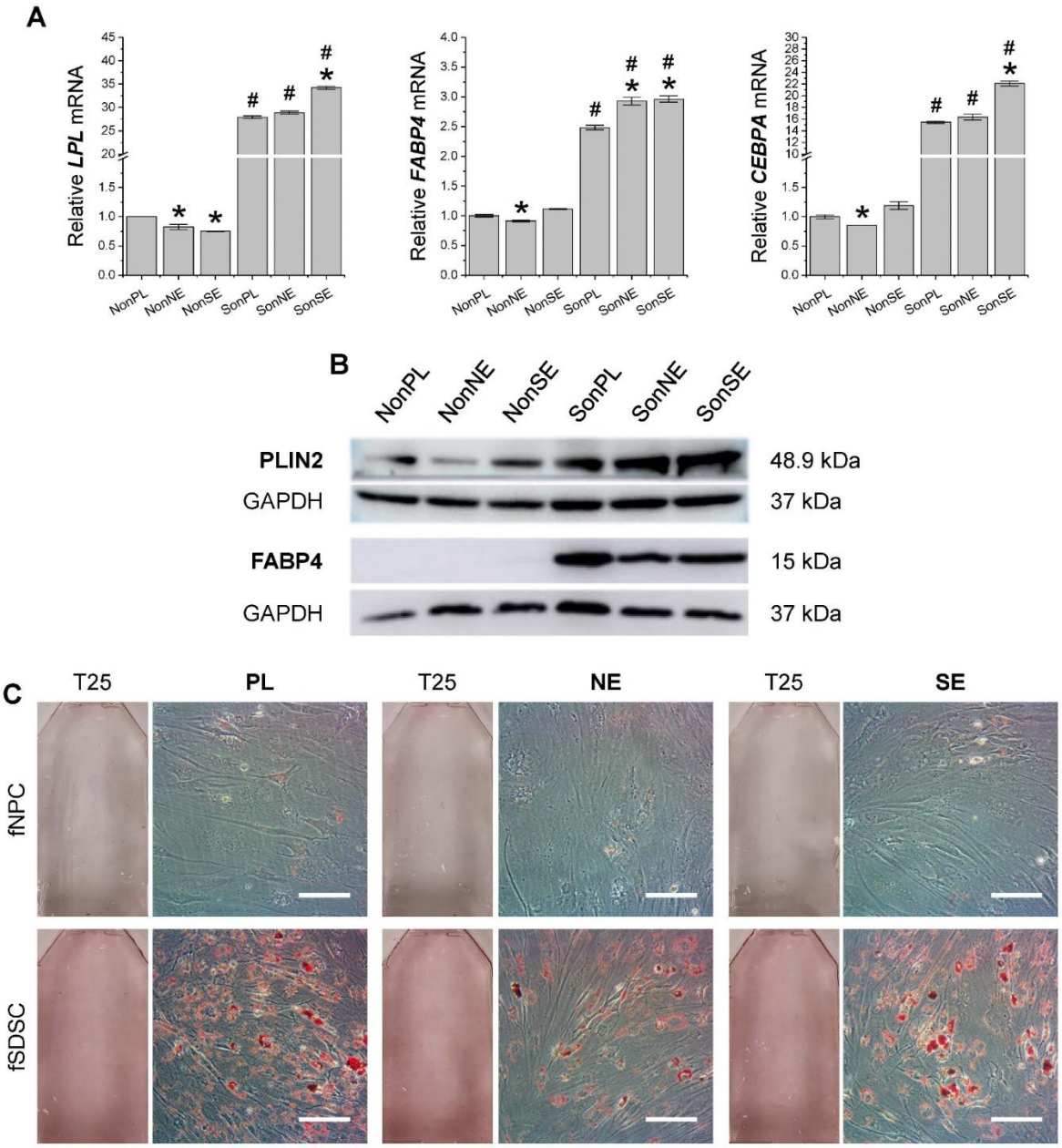

 doi:10.20944/preprints202312.1155.v1

Figure 4. Adipogenic evaluation of dECM expanded fetal MSCs. Following expansion on dECMs deposited by fNPCs (NE) or fSDSCs (S) or tissue culture plastic (PL), fNPCs (N) and fSDSCs (S) were incubated in adipogenic medium for 21 days. (**A**) TaqMan® real-time qPCR was used to evaluate adipogenic marker genes *LPL*, *FABP4*, and *CEBPA* of day 21 samples. *GAPDH* serves as the internal control. Data shown as a bar chart. * indicates a statistically significant difference from the corresponding PL group ($p < 0.05$). # indicates a statistically significant difference from the corresponding fNPC group ($p < 0.05$). (**B**) Western blot was used to evaluate adipogenic markers PLIN2 and FABP4 of day 21 samples. GAPDH serves as the internal control. (**C**) Oil Red O staining was used to detect lipid droplets of adipogenically induced cells in T25 flasks. Scale bar: 100 μm.

3.5. Osteogenic capacity of fetal stem cells after growth on dECMs

To characterize the osteogenic potential of fetal MSCs following expansion on dECMs, P5 fSDSCs and fNPCs grown on SECM and NECM for one passage were incubated toward osteogenesis for 21 days. qPCR data (**Figure 5A**) showed that, after osteogenic induction, fNPCs responded more significantly than the corresponding fSDSCs and exhibited higher expression of *BGLAP*, *ALPL*, and *COL1A1*. Compared to the Plastic group, dECM expanded fNPCs exhibited less expression of *BGLAP* and *COL1A1*, whereas dECM expanded fSDSCs displayed a slightly higher expression of *BGLAP* and *ALPL*. These mRNA data were in line with protein expression of ALPL by Western blot (**Figure 5B**) and calcium deposition by Alizarin Red S staining (**Figure 5C**).

Preprints (www.preprints.org) | NOT PEER-REVIEWED | Posted: 15 December 2023 doi:10.20944/preprints202312.1155.v1

Figure 5

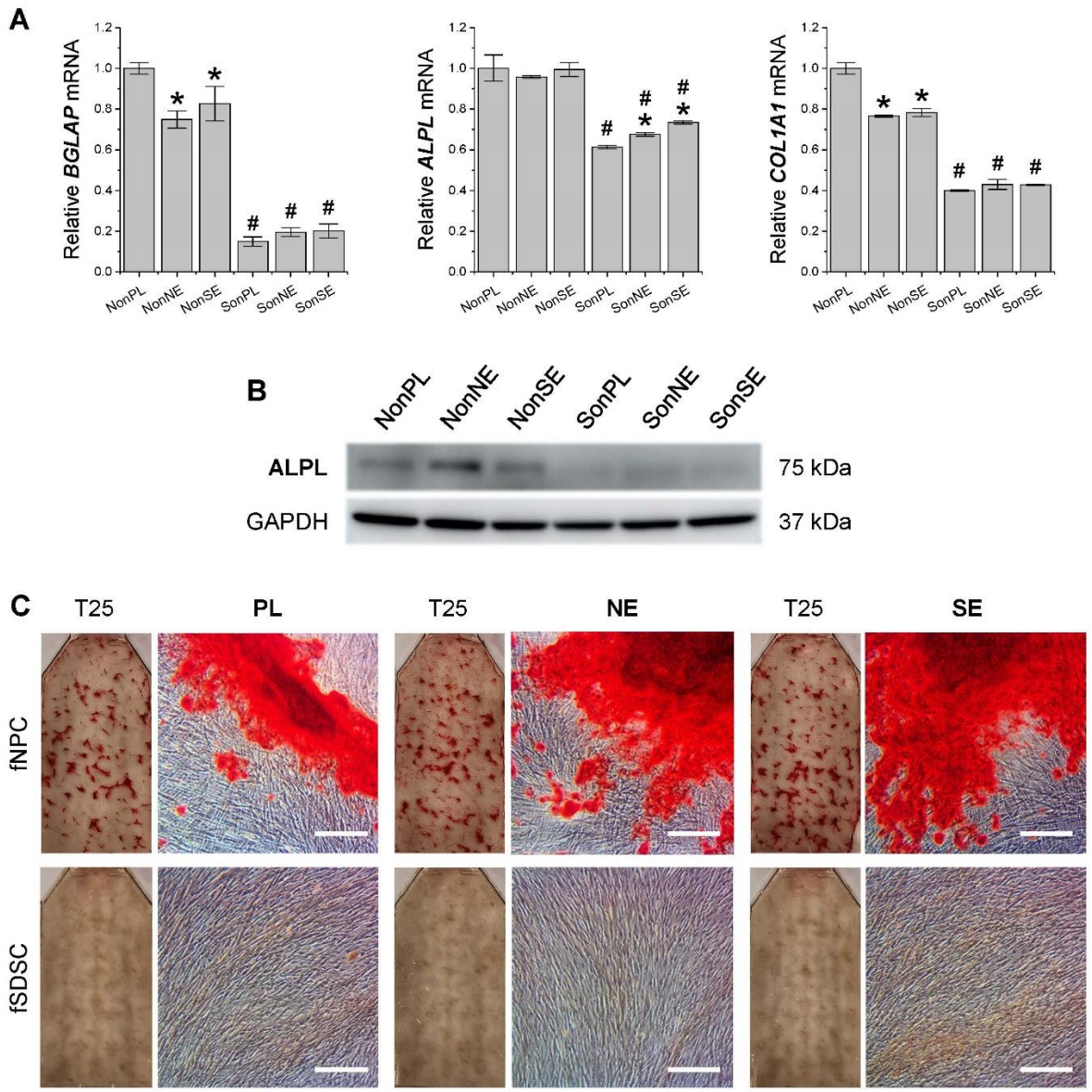

Figure 5. Osteogenic evaluation of dECM expanded fetal MSCs. Following expansion on dECMs deposited by fNPCs (NE) or fSDSCs (SE) or tissue culture plastic (PL), fNPCs (N) and fSDSCs (S) were incubated in osteogenic medium for 21 days. (**A**) TaqMan® real-time qPCR was used to evaluate osteogenic marker genes *BGLAP*, *ALPL*, and *COL1A1* of day 21 samples. *GAPDH* serves as the internal control. Data shown as a bar chart. * indicates a statistically significant difference from the corresponding PL group ($p < 0.05$). # indicates a statistically significant difference from the corresponding fNPC group ($p < 0.05$). (**B**) Western blot was used to evaluate osteogenic markers ALPL of day 21 samples. GAPDH serves as the internal control. (**C**) Alizarin Red S staining was used to detect calcium deposition of osteogenically induced cells in T25 flasks. Scale bar: 100 μm.

3.6. Major matrix protein expression in fetal stem cells, their matrix, and three-lineage differentiated cells

Immunofluorescence staining analysis showed that the NECM and SECM were positively stained for FN1, PLC, NID1, NID2, LAMA, and COL4. dECMs from both cells exhibited comparable density of staining in NID1, NID2, and COL4 except PLC intensely stained in SECM and FN1 and LAMA intensely stained in NECM (**Figure 6A**). The intensity of dECM staining was in line with qPCR data of expanded fetal stem cells, in which Plastic expanded fNPCs expressed more *FN1* and *LAMA5* and Plastic expanded fSDSCs expressed more *HSPG2* (**Figure 6B**). We found that, after chondrogenic

Preprints (www.preprints.org) | NOT PEER-REVIEWED | Posted: 15 December 2023 doi:10.20944/preprints202312.1155.v1

induction, *FN1* and *HSPG2* were upregulated and *NID1*, *NID2*, *LAMA5*, and *LAMB1* were downregulated in fNPCs, while *FN1* was upregulated and *HSPG2*, *NID1*, *NID2*, *LAMA5*, and *LAMB1* were downregulated in fSDSCs (**Figure 6B**). After adipogenic induction, *FN1*, *HSPG2*, and *LAMA5* were downregulated in fNPCs, while *NID2* was upregulated and *FN1*, *HSPG2*, *NID1*, *LAMA5*, and *LAMB1* were downregulated in fSDSCs (**Figure 6B**). After osteogenic induction, *FN1*, *HSPG2*, *NID1*, *NID2*, *LAMA5*, and *LAMB1* were upregulated in fNPCs, while *FN1*, *HSPG2*, *NID1*, *NID2*, and *LAMB1* were upregulated in fSDSCs (**Figure 6B**).

Figure 6

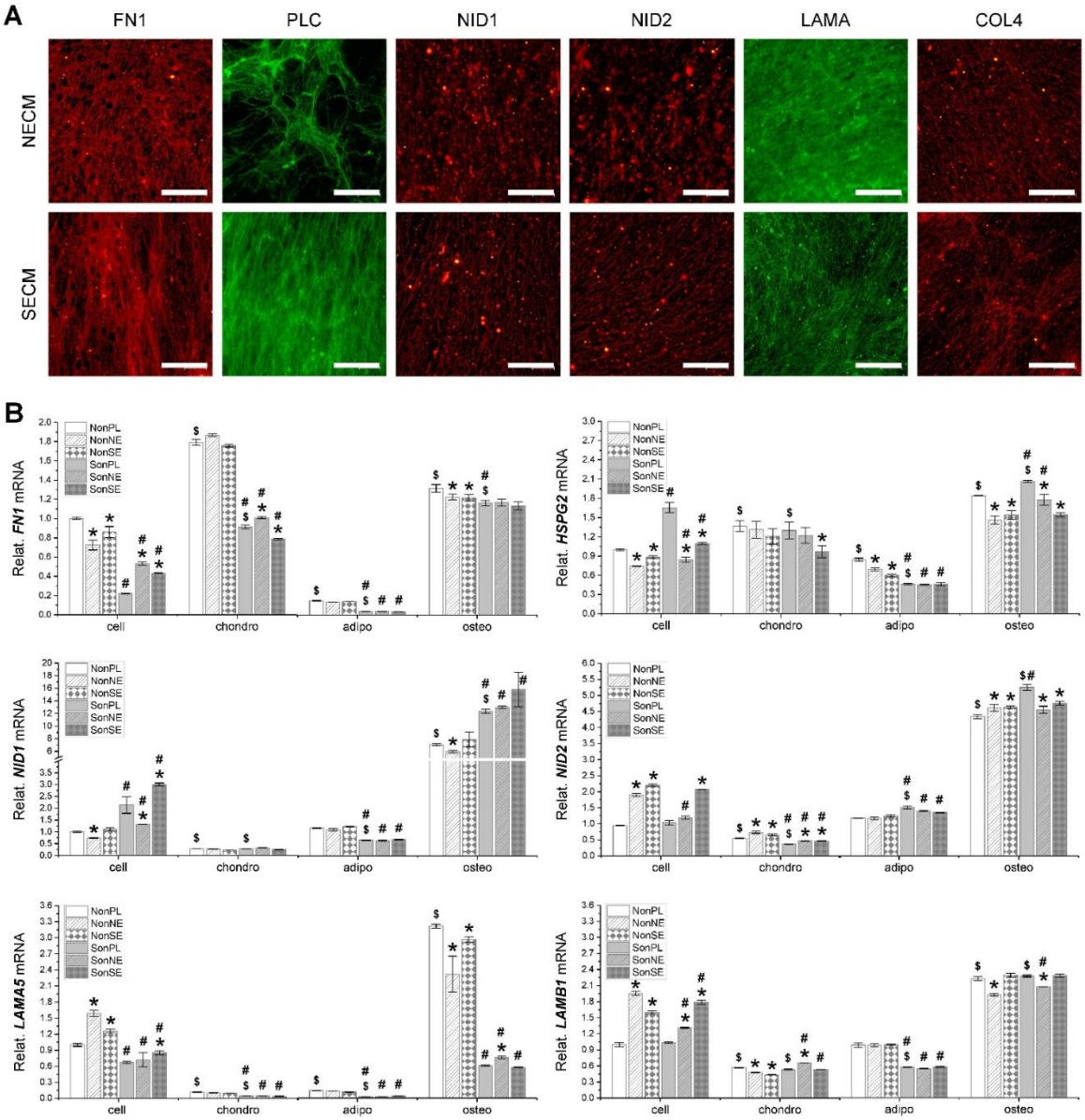

Figure 6. Major matrix protein expression in dECMs and differentiated fetal MSCs. (**A**) Immunofluorescence staining was used to detect expression of FN1, PLC, NID1, NID2, LAMA, and COL4 in dECMs deposited by fNPCs or fSDSCs. Scale bar: 100 μm. (**B**) TaqMan® real-time qPCR was used to evaluate mRNA levels of *FN1*, *HSPG2*, *NID1*, *NID2*, *LAMA5*, and *LAMB1* in expanded fetal MSCs and chondrogenically, adipogenically, and osteogenically induced cells. *GAPDH* serves as the internal control. Data shown as a bar chart. * indicates a statistically significant difference from the corresponding PL group ($p < 0.05$). # indicates a statistically significant difference from the

 doi:10.20944/preprints202312.1155.v1

corresponding fNPC group ($p < 0.05$). $ indicates a statistically significant difference from the corresponding PL-expanded cell samples ($p < 0.05$).

4. Discussion

Fetal MSCs are a promising approach to stem-cell therapy in regenerative orthopaedic medicine. The ex vivo environment, such as hypoxia, has been used to modulate the regenerative potential of fetal stem cells [22]. Knowing that a matrix microenvironment can influence the therapeutic potential of adult stem cells [10,23], in this study, we characterized two fetal cell types for their response to expansion on fetal dECM and subsequent differentiation capacity.

Compared to fNPCs, fSDSCs had higher overall expression of MSC surface markers, indicating greater cell proliferation capacity. Interestingly, fSDSCs grown on SECM exhibited an increased expression of CD73, SSEA4, and relative EdU incorporation but a decreased expression of CD90, CD105, and CD146. This finding is in line with previous reports, in which aSDSCs or fSDSCs grown on SECMs deposited by either aSDSCs or fSDSCs displayed a decrease in expression of CD90 and CD105 but an increase in SSEA4 [17,24]. An increase in expression of SSEA4 and relative EdU incorporation indicates that dECM expansion promoted MSC proliferation. The International Society for Cellular Therapy's 2006 conference defined CD73, CD90 and CD105 as surface markers for human MSCs [25]. Given this definition, it is challenging to interpret the similar trend in expression of MSC surface markers following dECM expansion with the dissimilar differentiation capacities shown in this study and others [26]. We also found that fetal cells responded differently to matrix rejuvenation in stemness gene expression. While fSDSCs are considered closer to MSCs and therefore more pluripotent than fNPCs, after dECM rejuvenation, interestingly, fNPCs displayed higher levels of pluripotency gene expression than fSDSCs.

Following expansion on Plastic flasks, different from aSDSCs losing their chondrogenic capacity during passaging from P3 to P5 [27], fSDSCs regained their chondrogenic potential from P2 to P9 [24]. dECM rejuvenation benefits adult MSCs grown on fetal dECM [17] and fetal MSCs grown on adult dECM [24] but not adult MSCs expanded on old dECM [18] and fetal MSCs expanded on fetal dECM [24]. In this study, fSDSCs grown on dECMs deposited by fSDSCs and fNPCs yielded 21-day pellets with decreased expression of *SOX9* and *ACAN* and increased expression of *COL2A1* and no significant difference of *PRG4* and *FBLN1*. In contrast, fNPCs grown on dECMs deposited by fSDSCs and fNPCs yielded 21-day pellets with increased expression of *ACAN*, *COL2A1*, and *PRG4*, and decreased expression of *COL1A1* and *COL10A1*. This finding indicates that, despite the fact that both are fetal cells, fNPCs (a progenitor cell for NP tissue) responded more positively to the rejuvenation of dECMs deposited by fSDSCs and fNPCs than fSDSCs. Interestingly, dECM rejuvenated fNPCs exhibited less response to both osteogenic and adipogenic induction compared to the Plastic group, which may be associated with the inherent nature of NPCs [28]. Compared to fNPCs, fSDSCs are closer to fetal MSCs. Despite less response to chondrogenic and osteogenic induction following dECM rejuvenation, under adipogenic induction, fSDSCs grown on dECM deposited by fSDSCs exhibited enhanced adipogenic capacity, evidenced by greater expression of *LPL*, *FABP4*, and *CEBPA* by qPCR analysis and PLIN2 and FABP4 by Western blot as well as more intensity of ORO staining indicating lipid droplets, which is in line with a previous report [24].

Major matrix components in dECMs and dynamic expression during three-lineage induction might contribute to lineage differentiation [29–32]. For instance, intense staining of fibronectin in NECM might contribute to greater levels of chondrogenic marker expression in the fNPC group compared to the fSDSC group [31,33]. Since fibronectin inhibits adipogenic differentiation [34–36], a lower level of fibronectin expression might contribute to higher levels of adipogenic differentiation in the fSDSC group. Enhanced chondrogenic capacity in dECM expanded fNPCs might also contribute by upregulation of LAMA5, which has been shown to favor chondrogenesis [30]. Interestingly, fSDSCs did not show a significant change in LAMA5 expression during osteogenic induction, indicating that LAMA5 might contribute to the osteogenic differentiation of fNPCs.

In summary, we demonstrated that matrix rejuvenation influences fetal stem cell stemness, proliferation, and differentiation capacities, establishing the potential of modulating matrix

environment to enhance fetal stem cell efficacy as a source for orthopaedic regenerative stem cell therapy and tissue engineering.

Author Contributions: Conceptualization, M.P.; methodology, Y.A.P.; validation, Y.A.P.; formal analysis, Y.A.P.; investigation, Y.A.P., J.P., and M.P.; resources, Y.A.P.; data curation, Y.A.P.; writing—original draft preparation, Y.A.P., J.P., and M.P.; writing—review and editing, Y.A.P. and M.P.; software, Y.A.P.; supervision, M.P.; project administration, M.P.; funding acquisition, M.P. All authors have read and agreed to the published version of the manuscript.

Funding: This research received no funding.

Institutional Review Board Statement: Ethical review and approval were waived for this study, due to commercial purchase of stem cells from unidentified donors.

Informed Consent Statement: Not applicable.

Acknowledgments: We thank Suzanne Danley for editing the manuscript.

Conflicts of Interest: The authors declare no conflict of interest.

References

1. Toh, W.S.; Foldager, C.B.; Pei, M, Hui JH. Advances in mesenchymal stem cell-based strategies for cartilage repair and regeneration. *Stem Cell Rev. Rep.* **2014**, 10, 686-696.
2. Li, J., Pei, M. Cell senescence: a challenge in cartilage engineering and regeneration. *Tissue Eng. Part B Rev.* **2012**, 18, 270-287.
3. Götherström, C., Ringdén, O., Westgren, M., Tammik, C., Le Blanc, K. Immunomodulatory effects of human foetal liver-derived mesenchymal stem cells. *Bone Marrow Transplant.* **2003**, 32, 265-272.
4. Le Blanc, K., Tammik, L., Sundberg, B., Haynesworth, S.E., Ringdén, O. Mesenchymal stem cells inhibit and stimulate mixed lymphocyte cultures and mitogenic responses independently of the major histocompatibility complex. *Scand. J. Immunol.* **2003**, 57, 11-20.
5. Montjovent, M.O., Bocelli-Tyndall, C., Scaletta, C., Scherberich, A., Mark, S., Martin, I., Applegate, L.A., Pioletti, D.P. In vitro characterization of immune-related properties of human fetal bone cells for potential tissue engineering applications. *Tissue Eng. Part A.* **2009**, 15, 1523-1532.
6. Allan, D.S. Using umbilical cord blood for regenerative therapy: Proof or promise? *Stem Cells* **2020**, 38, 590-595.
7. Guillot, P.V., Gotherstrom, C., Chan, J., Kurata, H., Fisk, N.M. Human first-trimester fetal MSC express pluripotency markers and grow faster and have longer telomeres than adult MSC. *Stem Cells* **2007**, 25, 646-654.
8. Li, J., He, F., Pei, M. Creation of an in vitro microenvironment to enhance human fetal synovium-derived stem cell chondrogenesis. *Cell Tissue Res.* **2011**, 345, 357-365.
9. Okamura, L.H., Cordero, P., Palomino, J., Parraguez, V.H., Torres, C.G., Peralta, O.A. Myogenic Differentiation Potential of Mesenchymal Stem Cells Derived from Fetal Bovine Bone Marrow. *Anim. Biotechnol*. **2018**, 29, 1-11.
10. Pei, M., Li, J.T., Shoukry, M., Zhang, Y. A review of decellularized stem cell matrix: a novel cell expansion system for cartilage tissue engineering. *Eur. Cell Mater*. **2011**, 22, 333-343; discussion 343.
11. Pei, M. Environmental preconditioning rejuvenates adult stem cells' proliferation and chondrogenic potential. *Biomaterials* **2017**, 117, 10-23.
12. Liu, X., Zhou, L., Chen, X., Liu, T., Pan, G., Cui, W., Li, M., Luo, Z.P., Pei, M., Yang, H., Gong, Y., He, F. Culturing on decellularized extracellular matrix enhances antioxidant properties of human umbilical cord-derived mesenchymal stem cells. *Mater. Sci. Eng. C Mater. Biol. Appl.* **2016**, 61, 437-448.
13. Pei, M., Zhang, Y., Li, J., Chen, D. Antioxidation of decellularized stem cell matrix promotes human synovium-derived stem cell-based chondrogenesis. *Stem Cells Dev.* **2013**, 22, 889-900.
14. Sun, Y., Yan, L., Chen, S., Pei, M. Functionality of decellularized matrix in cartilage regeneration: A comparison of tissue versus cell sources. *Acta Biomater*. **2018**, 74, 56-73.
15. Wang, Y., Chen, S., Yan, Z., Pei, M. A prospect of cell immortalization combined with matrix microenvironmental optimization strategy for tissue engineering and regeneration. *Cell Biosci.* **2019**, 9, 7.
16. Zhou, L., Chen, X., Liu, T., Zhu, C., Si, M., Jargstorf, J., Li, M., Pan, G., Gong, Y., Luo, Z.P., Yang, H., Pei, M., He, F. SIRT1-dependent anti-senescence effects of cell-deposited matrix on human umbilical cord mesenchymal stem cells. *J. Tissue Eng. Regen. Med.* **2018**, 12, e1008-e1021.
17. Li, J., Hansen, K.C., Zhang, Y., Dong, C., Dinu, C.Z., Dzieciatkowska, M., Pei, M. Rejuvenation of chondrogenic potential in a young stem cell microenvironment. *Biomaterials* **2014**, 35, 642-653.
18. Wang, Y., Hu, G., Hill, R.C., Dzieciatkowska, M., Hansen, K.C., Zhang, X.B., Yan, Z., Pei, M. Matrix reverses immortalization-mediated stem cell fate determination. *Biomaterials* **2021**, 265, 120387.

19. Jones, B.A., Pei, M. Synovium-derived stem cells: a tissue-specific stem cell for cartilage engineering and regeneration. *Tissue Eng. Part B Rev.* **2012**, 18, 301-311.
20. Chen S, Fu P, Wu H, Pei M. Meniscus, articular cartilage and nucleus pulposus: a comparative review of cartilage-like tissues in anatomy, development and function. *Cell Tissue Res*. **2017**, 370, 53-70.
21. Minogue, B.M., Richardson, S.M., Zeef, L.A., Freemont, A.J., Hoyland, J.A. Characterization of the human nucleus pulposus cell phenotype and evaluation of novel marker gene expression to define adult stem cell differentiation. *Arthritis Rheum.* **2010**, 62, 3695-3705.
22. Pei, Y.A., Pei, M. Hypoxia Modulates Regenerative Potential of Fetal Stem Cells. *Appl. Sci. (Basel)* **2022**, 12, 363.
23. Liu, C., Pei, M., Li, Q., Zhang, Y. Decellularized extracellular matrix mediates tissue construction and regeneration. *Front. Med*. **2022**, 16, 56-82.
24. Li, J., He, F., Pei, M. Chondrogenic priming of human fetal synovium-derived stem cells in an adult stem cell matrix microenvironment. *Genes Dis.* **2015**, 2, 337-346.
25. Dominici, M., Le Blanc, K., Mueller, I., Slaper-Cortenbach, I., Marini, F., Krause, D., Deans, R., Keating, A., Prockop, D.j., Horwitz, E. Minimal criteria for defining multipotent mesenchymal stromal cells. The International Society for Cellular Therapy position statement. *Cytotherapy* **2006**, 8, 315-317.
26. Lu, Z., Yan, L., Pei, M. Commentary on 'Surface markers associated with chondrogenic potential of human mesenchymal stromal/stem cells'. *F1000Res.* **2020**, 9, F1000 Faculty Rev-37.
27. He, F., Chen, X.D., Pei, M. Reconstruction of an in vitro tissue-specific microenvironment to rejuvenate synovium-derived stem cells for cartilage tissue engineering. *Tissue Eng. Part A*. **2009**, 15, 3809-3821.
28. Pei, Y.A., Mikaeiliagah, E., Wang, B., Zhang, X., Pei, M. The matrix microenvironment influences but does not dominate tissue-specific stem cell lineage differentiation. *Mater. Today Bio.* **2023**, 23, 100805.
29. Gao, G., Chen, S., Pei, Y.A., Pei, M. Impact of perlecan, a core component of basement membrane, on regeneration of cartilaginous tissues. *Acta Biomater*. **2021**, 135, 13-26.
30. Sun, Y., Wang, T.L., Toh, W.S., Pei, M. The role of laminins in cartilaginous tissues: from development to regeneration. *Eur. Cell Mater*. **2017**, 34, 40-54.
31. Wang, Y., Fu, Y., Yan, Z., Zhang, X.B., Pei, M. Impact of Fibronectin Knockout on Proliferation and Differentiation of Human Infrapatellar Fat Pad-Derived Stem Cells. *Front. Bioeng. Biotechnol.* **2019**, 7, 321.
32. Zhou, S., Chen, S., Pei, Y.A., Pei, M. Nidogen: A matrix protein with potential roles in musculoskeletal tissue regeneration. *Genes Dis.* **2021**, 9, 598-609.
33. Singh, P., Schwarzbauer, J.E. Fibronectin and stem cell differentiation - lessons from chondrogenesis. *J. Cell Sci.* **2012**, 125(Pt 16), 3703-3712.
34. Taleb, S., Cancello, R., Clément, K., Lacasa, D. Cathepsin s promotes human preadipocyte differentiation: possible involvement of fibronectin degradation. *Endocrinology* **2006**, 147, 4950-4959.
35. Uetaki, M., Onishi, N., Oki, Y., Shimizu, T., Sugihara, E., Sampetrean, O., Watanabe, T., Yanagi, H., Suda, K., Fujii, H., Kano, K., Saya, H., Nobusue, H. Regulatory roles of fibronectin and integrin α5 in reorganization of the actin cytoskeleton and completion of adipogenesis. *Mol. Biol. Cell* **2022**, 33, ar78.
36. Wang, Y., Zhao, L., Smas, C., Sul, H.S. Pref-1 interacts with fibronectin to inhibit adipocyte differentiation. *Mol. Cell Biol.* **2010**, 30, 3480-3492.